Titin in insect spermatocyte spindle fibers associates with microtubules, actin, myosin and the matrix proteins skeletor, megator and chromator

Lacramioara Fabian[1], Xuequin Xia[2], Deepa V. Venkitaramani[3], Kristen M. Johansen[3], Jørgen Johansen[3], Deborah J. Andrew[2] and Arthur Forer[1,*]

[1]Biology Department, York University, Toronto, ON, Canada
[2]Department of Cell Biology, The Johns Hopkins University School of Medicine, Baltimore, MD, USA
[3]Department of Biophysics, Biochemistry and Molecular Biology, Iowa State University, Ames, IA, USA
*Author for correspondence (e-mail: aforer@yorku.ca)

Accepted 24 April 2007
Journal of Cell Science 120, 2190-2204 Published by The Company of Biologists 2007
doi:10.1242/jcs.03465

Summary

Titin, the giant elastic protein found in muscles, is present in spindles of crane-fly and locust spermatocytes as determined by immunofluorescence staining using three antibodies, each raised against a different, spatially separated fragment of *Drosophila* titin (D-titin). All three antibodies stained the Z-lines and other regions in insect myofibrils. In western blots of insect muscle extract the antibodies reacted with high molecular mass proteins, ranging between rat nebulin (600-900 kDa) and rat titin (3000-4000 kDa). Mass spectrometry of the high molecular mass band from the Coomassie-Blue-stained gel of insect muscle proteins indicates that the protein the antibodies bind to is titin. The pattern of staining in insect spermatocytes was slightly different in the two species, but in general all three anti-D-titin antibodies stained the same components: the chromosomes, prophase and telophase nuclear membranes, the spindle in general, along kinetochore and non-kinetochore microtubules, along apparent connections between partner half-bivalents during anaphase, and various cytoplasmic components, including the contractile ring. That the same cellular components are stained in close proximity by the three different antibodies, each against a different region of D-titin, is strong evidence that the three antibodies identify a titin-like protein in insect spindles, which we identified by mass spectrometry analysis as being titin. The spindle matrix proteins skeletor, megator and chromator are present in many of the same structures, in positions very close to (or the same as) D-titin. Myosin and actin also are present in spindles in close proximity to D-titin. The varying spatial arrangements of these proteins during the course of division suggest that they interact to form a spindle matrix with elastic properties provided by a titin-like protein.

Key words: Crane flies, Locust, Titin, Spindle, Spindle matrix

Introduction

Titin, a protein of molecular mass of more than 3 MDa, is the third most abundant protein in muscle (after actin and myosin) and is responsible for much of the elasticity of myofibrils in various organisms (Granzier and Irving, 1995; Minajeva et al., 2001; Flaherty et al., 2002; Labeit et al., 2003; Neagoe et al., 2003; Tskhovrebova and Trinick, 2003; Miller et al., 2004; Hooper and Thuma, 2005). Titin molecules are associated with each thick filament in skeletal muscle, where they interact with myosin (Tskhovrebova and Trinick, 2003) and with a variety of sarcomere proteins (Tskhovrebova and Trinick, 2004; Lange et al., 2006). Each titin molecule extends from the M-band to the Z-line (Furst et al., 1988; Obermann et al., 1997; Gregorio et al., 1998), a distance of more than 1 μm. As the sarcomere increases in length, titin molecules stretch. Titin is responsible for most of the elastic force that returns stretched muscle to its resting length. When the muscle is stretched past overlap, titin is responsible for the thin filaments returning to interdigitate with thick filaments (Trombitás, 2000). Titin also is found in non-muscle contractile systems; for example, it is associated with sea-urchin zygote cytomatrix (Pudles et al., 1990), with erythrocyte membranes (Maruyama et al., 1977), with brush borders and stress fibers (Eilertsen and Keller, 1992; Eilertsen et al., 1994), with *Physarum* cytoplasmic matrix (Gassner et al., 1985), with microtubules (Pizon et al., 2002), with nuclear membranes (Zastrow et al., 2006) and with chromosomes, where it is thought to be involved in chromosomal elasticity (Machado et al., 1998; Houchmandzadeh and Dimitrov, 1999; Machado and Andrew, 2000a; Machado and Andrew, 2000b).

Mitotic spindles also have elastic components. In crane-fly spermatocyte spindles, for example, there are elastic 'tethers' between two arms of the separating anaphase chromosomes. These tethers provide backward forces on the chromosomes, as evidenced by backward movements across the equator when anaphase chromosome arms are severed with a laser microbeam (LaFountain et al., 2001) and by the entire chromosome moving backwards across the equator after UV microbeam irradiation of kinetochores alone or in combination with interzonal irradiation (Ilagan et al., 1997; Wong and Forer, 2004). In addition, the spindle itself may have elastic properties; when a UV microbeam severs all microtubules across a newt fibroblast spindle, the spindle shortens in the absence of microtubule

continuity, as if an elastic spindle matrix provides the continuity (Spurck et al., 1990). Furthermore, an elastic spindle matrix, in conjunction with other spindle forces, might be responsible both for the wobbling motion of the kinetochore stub and for the continued poleward motion of the chromosome after a UV microbeam severs a single kinetochore fiber in anaphase crane-fly spermatocytes (Pickett-Heaps et al., 1996; Forer et al., 2003). Direct evidence of a spindle matrix was provided by isolation of a protein (skeletor) from *Drosophila* cells. Skeletor localizes to a spindle-shaped structure coincident with spindle microtubules, but the skeletor spindle maintains its spindle shape even after spindle microtubules are experimentally removed (Walker et al., 2000). Another protein suggested as a structural component of the spindle matrix is lamin B, an intermediate filament present in the interphase nuclear lamina (Tsai et al., 2006). Because mitotic spindles also contain the muscle proteins actin and myosin (Forer et al., 2003; Silverman-Gavrila and Forer, 2003; Robinson and Snyder, 2005), which seem to be involved in force production in anaphase chromosome movement (Forer et al., 2003; Fabian and Forer, 2005; Fabian et al., 2007; Fabian and Forer, 2007), we thought that titin might be involved with spindle elasticity, as it is in muscle. Because spindle elasticity might be associated with a spindle matrix, we tested whether titin was present in spindles and whether it was associated with a spindle matrix.

We studied the localization of titin in crane-fly and locust spermatocytes using three different antibodies, each produced against spatially distinct domains of *Drosophila* titin (D-titin). As described in this report, staining for D-titin was found in the spindles of both species, in all stages, along the spindle fibers, and in positions similar to actin, myosin and the *Drosophila* spindle matrix protein skeletor. D-titin also was associated with structures that extend between partner chromosomes during anaphase. Our results suggest that D-titin associates with actin, myosin and *Drosophila* matrix proteins (skeletor, megator and chromator) and might provide elasticity to the spindle matrix.

Results

Staining of *Drosophila* embryos

We stained skeletal muscle in *Drosophila* embryos to confirm that the three anti-titin antibodies stain the same molecule. The Berkeley *Drosophila* genome project indicates that there are three distinct genes in the titin region: (1) *zormin* is predicted to encode a 2947-residue protein with eight immunoglobulin (Ig) repeat domains and with significant homology to both vertebrate and *C. elegans* titin; (2) *CG32307* is predicted to encode a 178-residue protein with no significant homology to any proteins or predicted ORFs in the NCBI database; (3) *sallimus/titin* is predicted to encode a 18,074-residue protein with 47 Ig domains, five fibronectin type three (FN3) repeat domains, two regions rich in the residues proline (P), glutamic acid (E), valine (V) and lysine (K) and with significant homology to vertebrate and *C. elegans* titin (Fig. 1A,B). Based on the orientation of the three predicted genes and the shared homology of zormin and sallimus/titin to titins from other species, we predict that *zormin*, *CG32307* and *sallimus/titin* are all part of the same gene. The near impossibility of obtaining full-length cDNA clones for transcripts larger than *sallimus/titin* and the existence of additional alternative consensus splice sites suggests that the *titin* gene may encode multiple splice forms, as has already been demonstrated with *kettin*, a shorter splice form from the *sallimus/titin* gene (Zhang et al., 2000; Machado and Andrew, 2000a). Using a subset of the alternative consensus splice sites, we created a composite *titin* transcript that spanned from the 5′ translation start site for *zormin* to the 3′ translation stop site of *sallimus/titin* and included a significant portion of the ORFs from the three adjacent genes. We generated antisera to both a fragment of the predicted *zormin* ORF (anti-52) and to two fragments of the predicted *sallimus/titin* ORF (anti-KZ and anti-56). Anti-52 and anti-KZ antibodies had identical staining patterns in *Drosophila* embryos, with staining in the somatic, visceral and pharyngeal muscle, as well as in the apodemes (muscle attachment points) (Fig. 1C). Anti-56 antibody had nearly the same staining pattern, except staining in the visceral mesoderm was significantly reduced (Fig. 1C). Since the three antibodies were generated to distinct fragments of titin yet stain the same cellular components in *Drosophila* embryos, the antibodies stain the same molecule, presumably titin, consistent with all three predicted ORFs being encoded by a single large transcript. Thus staining with the three antibodies can be used to identify D-titin in cells.

Each of the three antibodies stains the same cellular components in crane-fly and locust spermatocytes, at positions very close together, as we describe in detail below.

Staining of insect myofibrils

As a further control that the different anti-D-titin antibodies stained titin-like components, we determined the localization of the three antibodies against D-titin in the sarcomeres of glycerinated insect myofibrils. For each antibody, the patterns of staining varied with sarcomere length. At any given sarcomere length the different antibodies stain somewhat differently: the Z-line, identified from DIC and phase-contrast images (Fig. 2A), stains prominently at shorter lengths, but the relative staining of non-Z-line components differs with the different antibodies (Fig. 2B-D). At longer sarcomere lengths the Z-line material redistributes to the rest of the sarcomere (anti-KZ), and may even leave the Z-line (anti-56) or remains prominent as the non-Z-line staining redistributes (anti-52). These results are consistent with each antibody staining a titin-like protein in which different epitopes respond differently to stretch, by changing positions, and/or by becoming more or less exposed as sarcomeres change length (Itoh et al., 1988; Horowits et al., 1989; Linke et al., 1999; Neagoe et al., 2003).

Western blotting and mass spectrometry analysis

To further test that the different antibodies stained titin-like proteins we used vertical agarose gel electrophoresis and immunoblotting (Warren et al., 2003) to characterize the antibodies. In 1% agarose gels, the myosin runs with the front (Warren et al., 2003) and the D-titin-like protein from insect muscle migrated as several bands with molecular masses ranging between those of rat titin (3000-4000 kDa) and rat nebulin (600-900 kDa) (Fig. 3A). These bands appeared to be the same as ‘mini-titin’, which was isolated from locust and other insect muscle by Nave and Weber (Nave and Weber, 1990). In western blots, all three anti-D-titin antibodies bound proteins with a molecular mass greater than that of nebulin, within the range of the ‘mini-titin’ (Fig. 3B) (Nave and Weber, 1990).

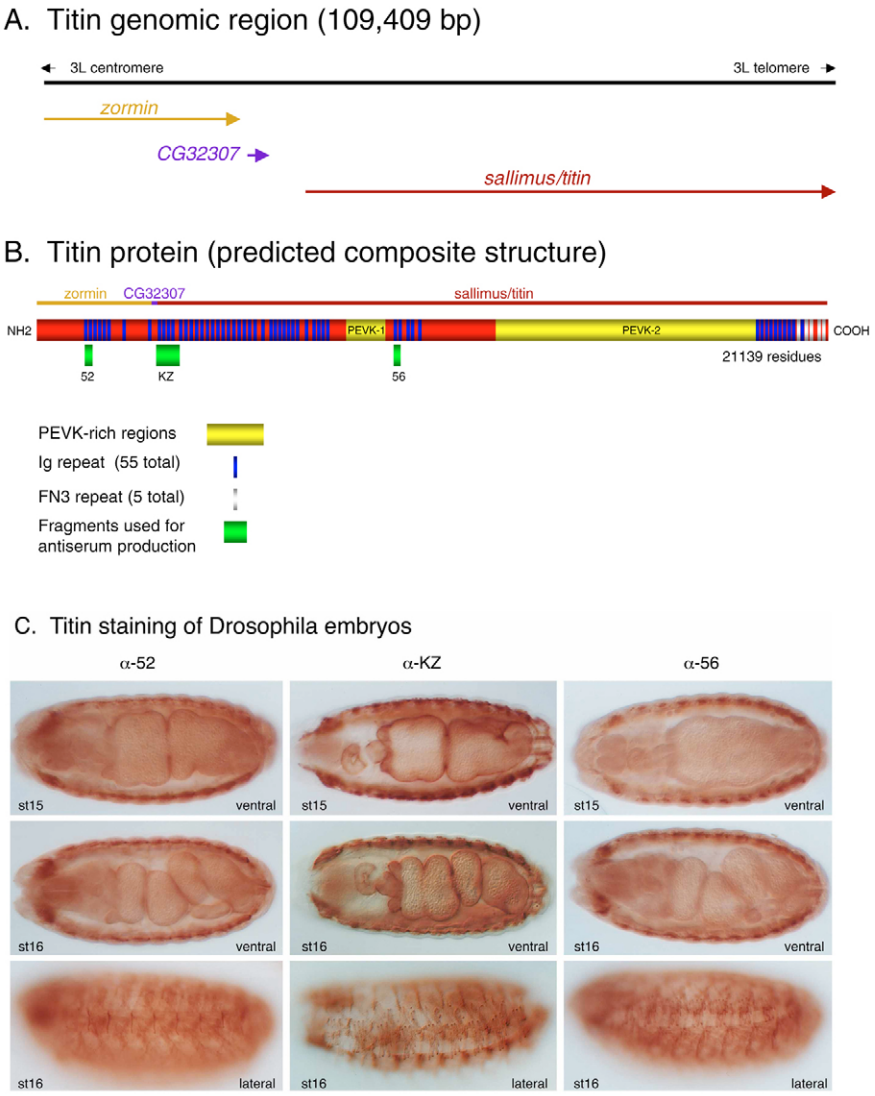

Fig. 1. (A) The titin genomic region spans from the 5′ end of the predicted *zormin* ORF through the 3′ end of the predicted *sallimus/titin* ORF. Both of the ORFs predicted from *zormin* and *sallimus/titin* have significant homology to vertebrate titin and to the multiple *C. elegans* titin-like proteins. (B) The domain structure of the predicted composite titin protein, which would include 21139 residues, contains 55 immunoglobulin repeats (Ig; blue), five fibronectin type-3 repeats (FN3; silver) and two extended domains rich in Pro, Glu, Val and Lys (PEVK-1 and PEVK-2; yellow). Polyclonal antiserum was generated to three non-overlapping fragments from the composite protein (52, KZ and 56; green). The colored line above the domain structure indicates which regions of the protein are encoded by the three Celera Genomics Predicted genes: *zormin* (yellow), *CG32307* (purple) and *sallimus/titin* (red). (C) *Drosophila* embryos stained with antisera generated to protein fragments corresponding to the *zormin* coding region (anti-52) and to the N-terminal region of the *sallimus/titin* coding region (anti-KZ) show identical patterns of accumulation, with staining in the skeletal, pharyngeal and visceral muscle, as well as in the muscle attachment points, known as apodemes (left and middle panels). *Drosophila* embryos stained with antiserum raised against a more central fragment of the *sallimus/titin* coding region show the same pattern of accumulation except that staining is not detected to high levels in the visceral muscle (right panels).

Mass spectrometry analysis was performed at the Centre for Research in Mass Spectrometry (York University, Toronto, Canada) on bands cut out of agarose gels of insect muscle extracts. Ten of the most intense peaks observed in the MS scan were picked for fragmentation by tandem mass spectrometry analysis (MS/MS) (Shevchenko et al., 1996; Jacobs et al., 2006). Three peptides matched gi/91076016 with a score of 61. This sequence when aligned using NCBI BLAST algorithm matched the titin protein from several organisms, including *Drosophila*. Thus, titin is present in muscle, and the antibodies recognise this protein in western blots.

Lysis and fixation procedures do not affect protein distribution

We wanted to verify that the methods used to prepare the cells did not affect protein distribution, especially because the D-titin staining of distinct subcellular structures in crane-fly and locust spermatocytes that we observed has not been described previously. Therefore we tested several different preparation protocols described in the Materials and Methods section. With all the protocols used, the D-titin staining pattern was the same as with our typical preparation protocol (e.g. anti-KZ in Fig. 4C first panel vs second panel). Thus, we are confident that the staining patterns reflect the actual distribution of the D-titin epitopes. As a further control, we omitted the primary antibody in some of the preparations, after which no staining was observed. To ensure that cross-talk between channels did not contribute to the staining we attribute to D-titin, we single-stained with anti-D-titin antibody only; the results were identical to those seen in double-stained preparations. Furthermore, the staining patterns were similar regardless of the order of staining in double-stained preparations and regardless of the wavelength of fluorochrome attached to the secondary antibody.

The various control experiments described above indicate that the use of the three antibodies against D-titin together identifies a titin-like protein in crane-fly and locust spermatocytes, and that the preparation procedures do not alter D-titin localization. We now describe in detail the localization of D-titin in insect spermatocytes.

D-titin distribution in insect spermatocytes

In dividing cells, antibodies against D-titin stained the same structures in crane flies and in locusts with a similar punctate

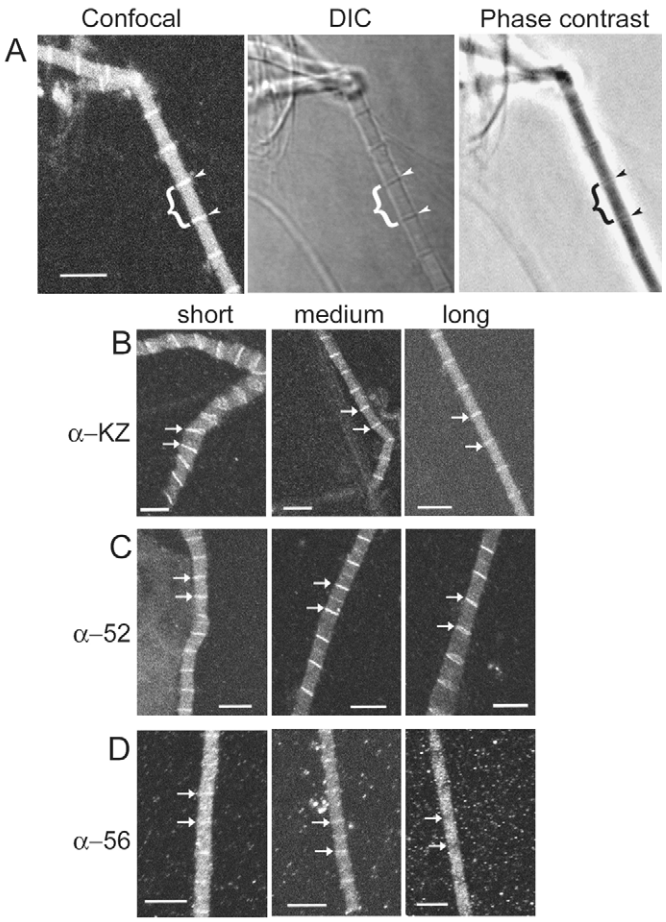

Fig. 2. Distribution of anti-D-titin antibodies in glycerinated myofibrils from crane-fly flight muscle. (A) An example of the method we used to identify Z-lines in confocal images. The same myofiber is illustrated in a phase-contrast image, a DIC image and a confocal microscope image. The brackets show the same sarcomere in the three images and the arrowheads point to Z-lines, which delimitate the sarcomere. (B-D) In general, the Z-lines (arrows), identified from corresponding DIC and phase-contrast images, are brightly stained. There is diffuse staining in between, along the length of the sarcomere. The staining patterns of all three antibodies vary with the sarcomere length, as described in text. Bars, 5 μm.

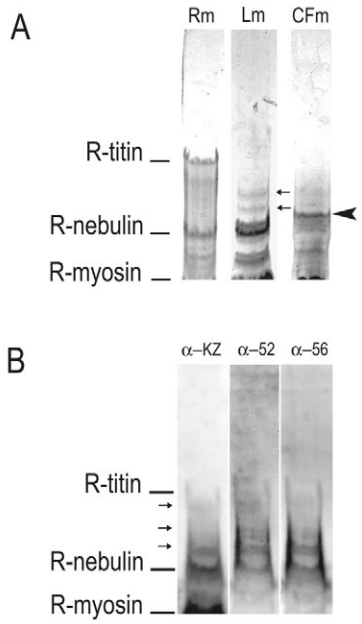

Fig. 3. (A) Coomassie-Blue-stained agarose gel of rat muscle (Rm), locust muscle (Lm) and crane-fly muscle (CFm). The highest molecular mass components in crane-fly and locust muscle (arrows) run about half-way between rat titin and rat nebulin, similarly to the doublets of mini-titin (Nave and Weber, 1990). The arrowhead indicates the band used for mass spectrometry analysis. (B) Western blots of locust muscle probed with three anti-D-titin antibodies. All three antibodies stain the highest molecular weight bands (arrows) seen in the Coomassie-Blue-stained gels, corresponding to mini-titin, as indicated by their position relative to rat titin and rat nebulin, which act as markers (Warren et al., 2003). Myosin runs with the Bromophenol Blue dye front and is at the bottom of the lanes. The proteins were separated on agarose gels, transferred to PVDF membrane and visualized with ECL. The same membrane was used for all three anti-D-titin antibodies (after stripping and reprobing).

pattern of distribution in discrete dots. The positions of the three antibodies were close, but not exactly the same, which is expected, given the size of this giant molecule and the fact that the three D-titin fragments used to generate the antisera are separate from each other in the protein.

In interphase cells, D-titin staining is localized mainly to the nucleus and the nucleolus, but there was some (weaker) staining of the cytoplasmic cytoskeleton (data not shown). In prophase, D-titin staining was found in the chromosomes, in high concentration at their peripheries (Fig. 4A, arrowheads in left and right panels), and with a uniform, diffuse distribution in the rest of the chromosomes (Fig. 4A,B); in the nuclear membrane (Fig. 4A, arrows); along the cytoplasmic astral arrays (Fig. 4A, left panel); and at a high concentration in an unidentified cytoplasmic body. During prometaphase, D-titin stained the entire spindle area with equal distribution along both the kinetochore fibers and the rest of the spindle fibers, defining a spindle area with brighter staining at the poles. D-titin staining also was in the chromosomes at high levels at this stage (Fig. 4C,D), but without being concentrated at their peripheries. By metaphase, D-titin staining co-localized with tubulin staining along the kinetochore microtubules and, to a lesser degree, along other microtubules in the spindle (Fig. 5). D-titin staining was also found at the poles (but not along astral microtubules) and in the chromosomes (Fig. 5A,B). In metaphase, chromosome staining was slightly weaker than in prophase and, as determined by quantitative analysis of staining intensities in crane-fly spermatocytes, was about the same intensity as or slightly greater intensity than in the spindle. During anaphase, the D-titin distribution followed the kinetochore microtubules (Fig. 6A,B), which shorten during this phase; all three antibodies co-localized with tubulin along the kinetochore fibers (Fig. 6C-F), and, in general, there was less co-localization along the other microtubules that make up the spindle (Fig. 6E,F). During anaphase, D-titin staining was still present in the chromosomes (Fig. 6A,B) and appeared to connect (as a sequence of 'dots') the trailing arms of the separating half-bivalents (Fig. 6A, insert). In telophase or

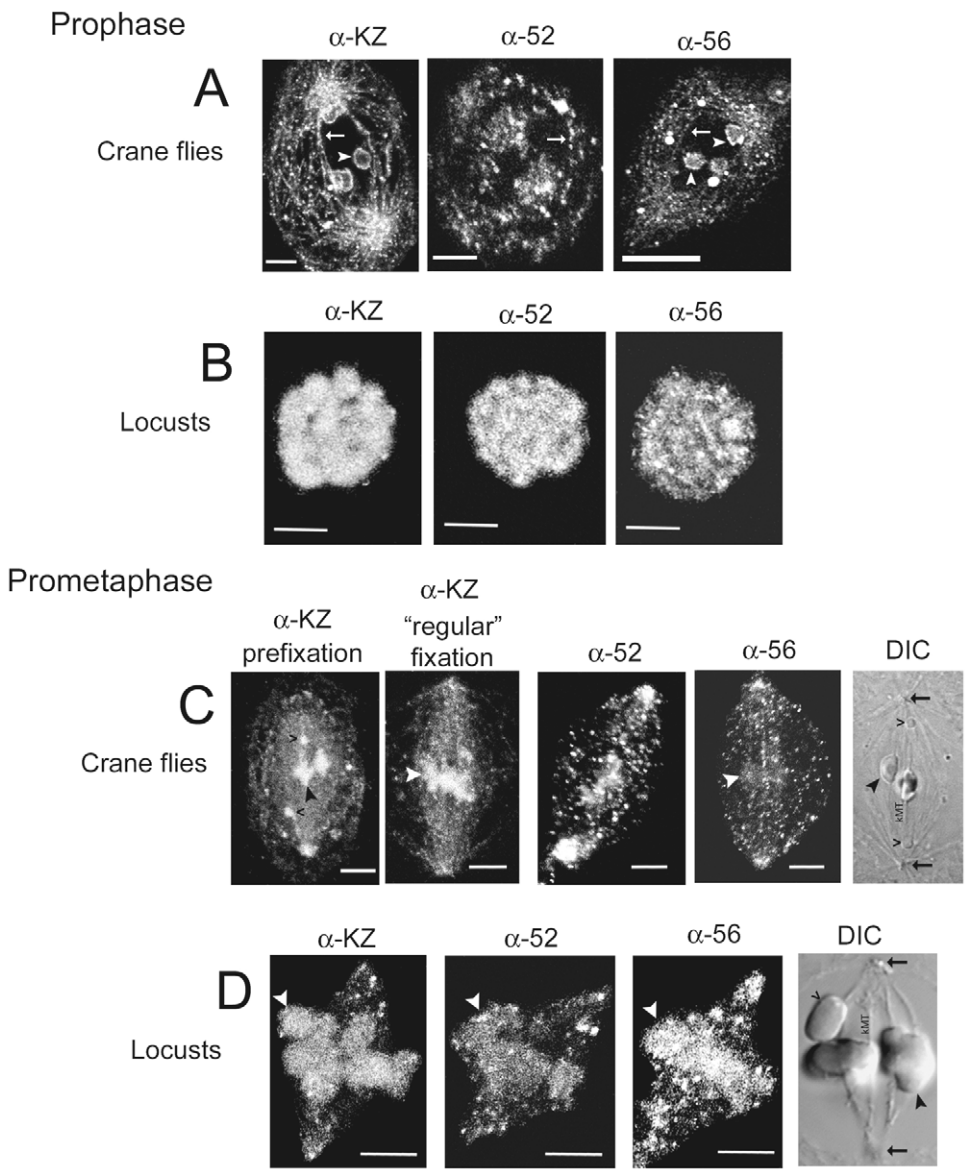

Fig. 4. D-titin distribution in prophase and prometaphase insect spermatocytes. (A) Distribution of three anti-D-titin antibodies in prophase crane-fly spermatocytes. These antibodies stain the nuclear membrane (arrow), the periphery of chromosomes (arrowheads) and the body of chromosomes. No staining of the periphery of the chromosomes was observed with the anti-52 antibody. Also, the staining of the nuclear membrane with anti-52 is less intense than with the other two antibodies (arrow in the central panel) and was seen in a small percentage of cells only. (B) Distribution of anti-KZ, anti-52 and anti-56 antibodies in prophase locust spermatocytes, illustrating staining of chromosomes. (C) Distribution of anti-KZ, anti-52 and anti-56 antibodies in prometaphase crane-fly spermatocytes. Left panel illustrates a cell fixed and lysed with a different protocol than our regular one: the lysis and fixation were done simultaneously, as one step, as described in the Materials and Methods. (D) Distribution of anti-KZ, anti-52 and anti-56 antibodies in prometaphase locust spermatocytes. Arrowheads in C and D indicate autosomal bivalents and open arrowheads indicate sex chromosomes. kMT indicates kinetochore microtubules. The arrows in the DIC pictures indicate the spindle poles. The DIC pictures are of lysed cells not illustrated in the fluorescent images. Bars, 5 μm.

cytokinesis, D-titin antibodies stained mid-body microtubules (Fig. 6G,H), the two newly forming nuclei and their nascent membranes (Fig. 6G, arrows in left and right panels), and, to a lesser extent, the contractile ring (Fig. 6G,H). In some cases, D-titin staining was seen in the flagella at the poles of the spindle (Fig. 6G, arrowhead and Fig. 7C), in sperm tails, and in an unidentified compact body in the cytoplasm, present close to the spindle.

The three different antibodies against D-titin stained the same spindle components. With all possible combinations of anti-D-titin antibodies (Fig. 7), the different antisera stained separate positions along the spindle fibers; they appear in merged images as separate red vs green 'dots' (Fig. 7B,D) about 1.5-2 μm apart, centre-to-centre, when measured along the length of the kinetochore fiber, or about 0.2 μm apart when the two closest red/green dots were measured slightly obliquely to the length of the kinetochore spindle fiber (Fig. 7). Thus at every stage of division, in each organelle they stain, their positions are very close, but they do not superimpose exactly, except at the spindle poles and in the chromosomes, where there is a higher concentration of D-titin.

In some experiments, RNase was added to the primary and secondary antibody solutions to test whether this might change the appearance of spindle staining, because Machado et al. (Machado et al., 1998) treated their cells with RNase and saw no spindle staining with the anti-KZ antiserum. The RNase treatment caused a dramatic increase in anti-KZ staining of chromosomes compared with spindle fibers (Fig. 7F, arrow and arrowhead in left panel), although anti-56 staining was unchanged after RNase treatment (Fig. 7F, right panel).

Comparison of intensity of D-titin staining in insect spermatocytes to staining in myofibers

When compared with the staining intensity of myofibers, all three anti-D-titin antibodies stained spermatocytes at about the same relative intensity. During interphase/prophase, the fluorescence from the chromosomes was considerably stronger than that of myofiber Z-lines in the same preparation. In

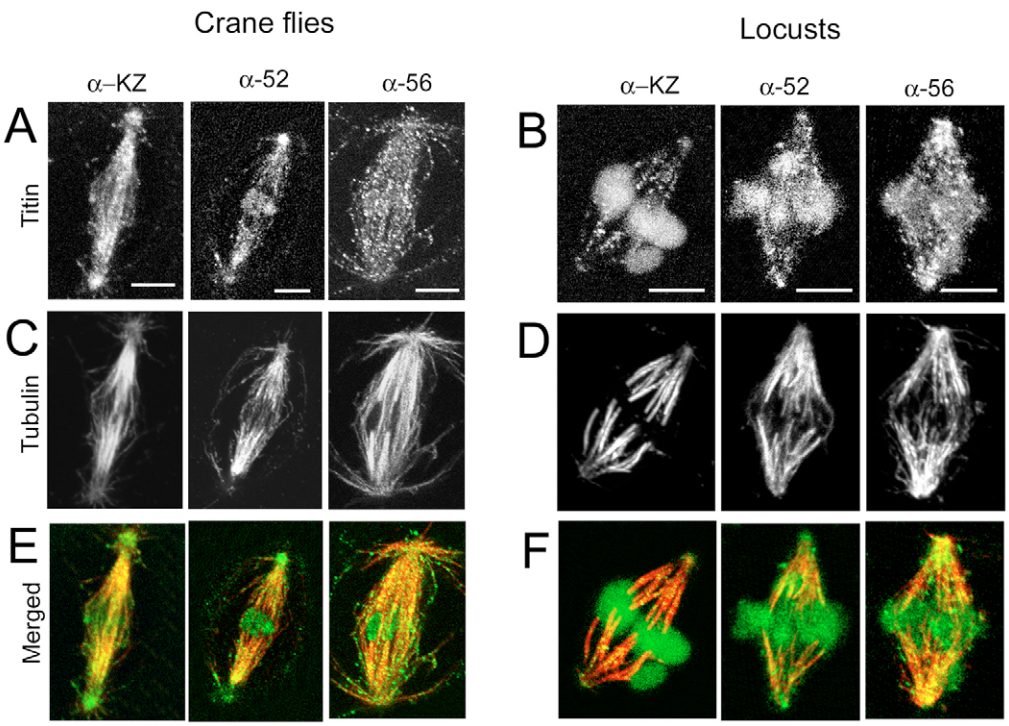

Fig. 5. D-titin distribution in metaphase insect spermatocytes. Distribution of anti-KZ, anti-52 and anti-56 antibodies against D-titin (green) in (A) metaphase crane-fly spermatocytes and (B) metaphase locust spermatocytes. Distribution of tubulin (red) in (C) crane-fly spermatocytes and in (D) locust spermatocytes. (E,F) Merged channels of D-titin and tubulin (yellow-orange color indicates co-localization). Bars, 5 μm.

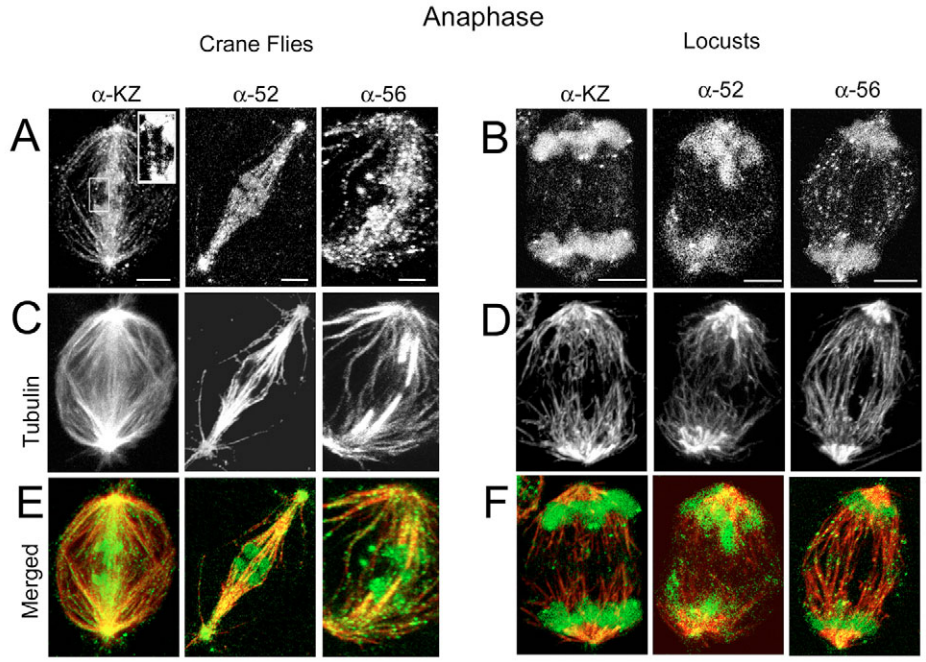

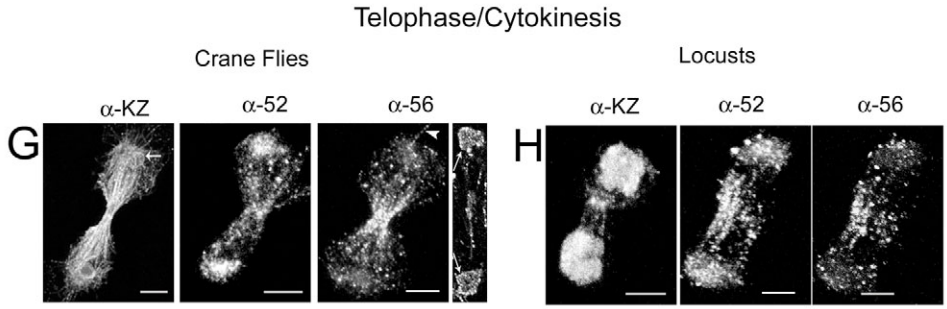

Fig. 6. D-titin distribution in anaphase and telophase insect spermatocytes. (A,B) Distribution of anti-KZ, anti-52 and anti-56 antibodies against D-titin (green) in anaphase crane-fly spermatocytes (A) and anaphase locust spermatocytes (B). (C,D) Distribution of tubulin (red) in crane-fly spermatocytes (C) and locust spermatocytes (D). (E,F) Merged channels of D-titin and tubulin. Insert in A, left panel, is an enlarged detail of the boxed region, showing punctate D-titin connections between the separating half-bivalents. (G,H) Distribution of anti-KZ, anti-52 and anti-56 antibodies against D-titin in telophase crane-fly spermatocytes (G) and in telophase locust spermatocytes (H). D-titin is associated with mid-body microtubules, with chromatin, with the nascent nuclear membranes (arrows in G, left and right panel) and with the flagella (arrowhead in G, third panel). Bars, 5 μm.

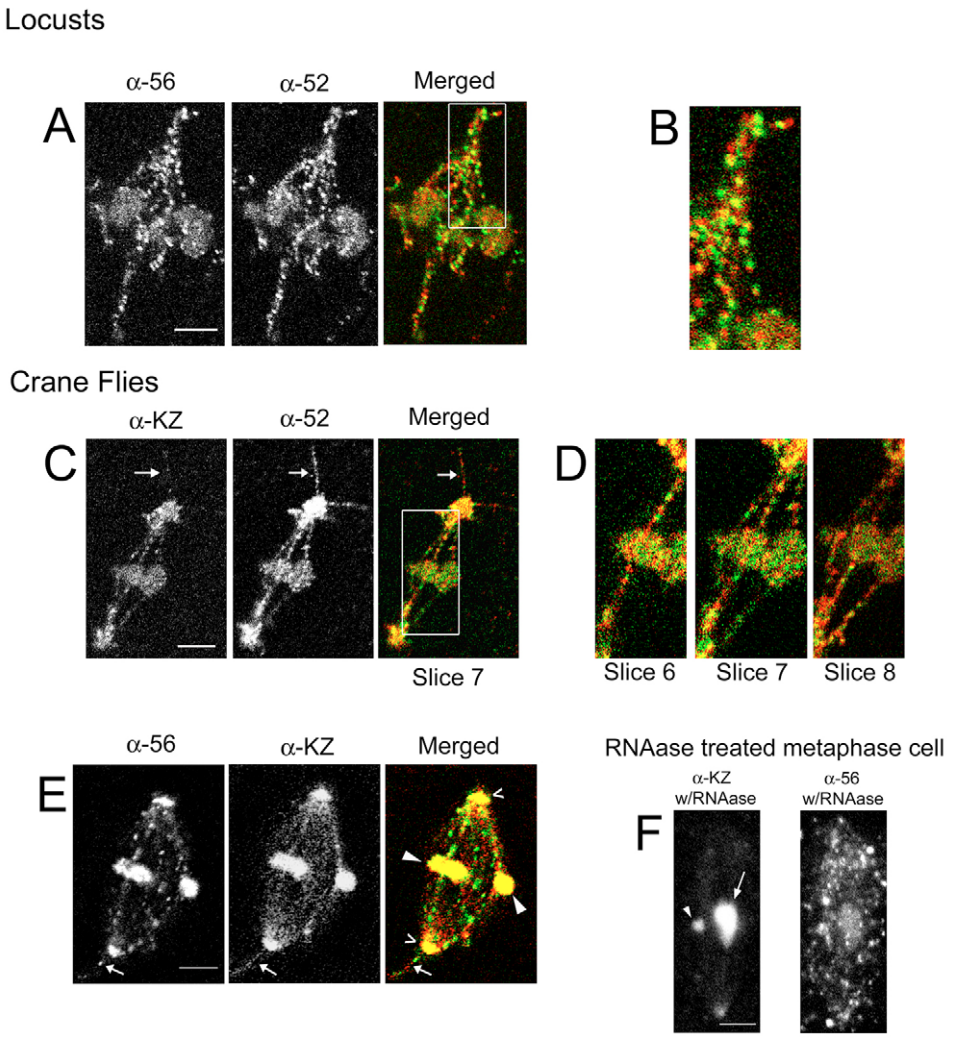

Fig. 7. Two-by-two combinations of anti D-titin antibody staining in metaphase insect spermatocytes. (A) One confocal slice showing the distribution of anti-56 antibody (green) and anti-52 antibody (red) staining in metaphase locust spermatocytes. The two antibodies show a punctate distribution of D-titin, which is localized in each case along the kinetochore spindle fibers (merged image) with little co-localization (yellow-orange color). (B) Enlarged region of the boxed region marked in A, showing the regular, punctate distribution of anti-56 antibody (green) and anti-52 antibody (red) staining and the co-localization of different D-titin fragments along one kinetochore spindle fiber. (C) One confocal slice showing the distribution of anti-KZ antibody (green) and anti-52 antibody (red) staining in metaphase crane-fly spermatocytes. The two antibodies show the same pattern of punctate distribution as in A and localize along the kinetochore spindle fibers (merged image), with little co-localization. (D) Enlarged details of the boxed region in C, showing the regular, punctate distribution of anti-KZ antibody (green) and anti-52 antibody (red) staining and the co-localization (yellow-orange) along one kinetochore spindle fiber. Three consecutives slices illustrate their spatial localization in the *Z*-axis. (E) Distribution of anti-56 antibody (green) vs anti-KZ antibody (red) in a metaphase crane-fly spermatocyte. The two antibodies show the same pattern of punctate distribution as in A and C and localize along the kinetochore spindle fibers (merged image), with little co-localization except in the chromosomes (arrowheads) and at the poles (open arrowheads). The arrows indicate a flagellum extending from a spindle pole. (F) RNase treatment of crane-fly spermatocytes during the staining protocol resulted in increased chromosomal staining with anti-KZ antibody, thus masking the spindle staining (left panel) whereas anti-56 antibody staining remained unchanged, both in its localization and intensity (right panel) (cf. Fig. 4A, untreated). Both panels depict the same cell. Arrowhead indicates a sex chromosome and arrow indicates an autosomal bivalent. Bars, 5 μm.

metaphase and anaphase spermatocytes, all three antibodies stained kinetochore fibers to the same extent when compared with staining of myofiber Z-lines; average gray scale values along the lengths of kinetochore fibers were 50-60% of those of myofiber Z-lines and maximum values (i.e. of the discrete 'dots') were 85-90% of the myofiber Z-lines. Metaphase and anaphase chromosomes stained at about the same intensities as myofiber Z-lines. Thus, there were considerable amounts of D-titin staining in both kinetochore fibers and chromosomes.

Comparison of D-titin staining in crane flies to staining in locusts

Generally, crane-fly and locust spermatocytes had very similar distributions of D-titin throughout meiosis, but there were several differences. Generally, chromosomes in locust spermatocytes stained with higher intensities than chromosomes in crane-fly spermatocytes; less D-titin staining was observed at the poles in locust metaphase/anaphase spermatocytes compared with crane-fly spermatocytes (Fig. 4C,D); the asters were not stained in locust spermatocytes (Fig. 5E,F); neither cortex nor nuclear membrane staining was observed in locust spermatocytes; the anti-D-titin antibodies also stained the nuclear membrane and various cytoplasmic components in crane-fly spermatocytes but not in locust spermatocytes (Fig. 4A,B).

D-titin distribution compared with myosin and actin distributions

To understand how D-titin in spindles might relate to other muscle proteins found in spindles, we compared the patterns of distribution of D-titin (using anti-KZ antibody), myosin and actin. During all phases of mitosis, all three proteins were associated with the same spindle structures (chromosomes, non-kinetochore microtubules, kinetochore microtubules, poles, nuclei, sex chromosomes and their kinetochore microtubules), but not always in exactly the same positions. All of them were present in spindle fibers, where each co-localized with tubulin, but they were organized differently.

D-titin and myosin staining were found in the nucleus (chromosomes) in prophase cells, in very close proximity, in both crane-fly and locust spermatocytes; the chromosomes seemed to include evenly distributed molecules of myosin and D-titin. In prometaphase/metaphase and anaphase D-titin and myosin staining co-localized at the poles and in the chromosomes; they were close together along the kinetochore fibers, appearing as red or green (single stained) or yellow (co-stained) dots, parallel to and alternating along the long axis of the spindle, in very close proximity, but not forming a continuous filament (Fig. 8A,C). In anaphase, both proteins were also present in the interzone, along the structures between the separating half-bivalents, in positions very close to each other, with red and green dots closely spaced, almost touching, at an oblique axis to the long axis of the spindle (Fig. 8B). In cytokinesis, D-titin and myosin staining co-localized in the new nuclei and in the incipient nuclear membranes (data not shown), along mid-body microtubules, in the 'mitochondrial sheath' around the spindle, and in the contractile ring (data not shown).

Actin and D-titin were in close proximity at all stages, in both crane-fly and locust spermatocytes (Fig. 9). In prophase, there was no D-titin staining found in the cortex and actin co-localized with D-titin only in the chromosomes (Fig. 9D), although actin staining of chromosomes was weak relative to the cortex and cytoplasmic structures in this stage. In prometaphase, actin and D-titin staining was found in the chromosomes (Fig. 9A, arrows) and along the kinetochore spindle fibers, where D-titin was apparent as very fine dots along the continuous actin filaments. By metaphase, when the kinetochore fibers are thicker, the D-titin staining was punctate along actin in the kinetochore fibers (Fig. 9B,E), and was also found in the chromosomes (Fig. 9B,E arrows). In anaphase, D-titin and actin were closely associated along the spindle fibers, at the poles (Fig. 9C, arrowheads), in the chromosomes (Fig. 9C, arrows) and in the interzone (Fig. 9C, open arrowheads). These data suggest that D-titin, myosin and actin might interact in insect spindles during all stages of division.

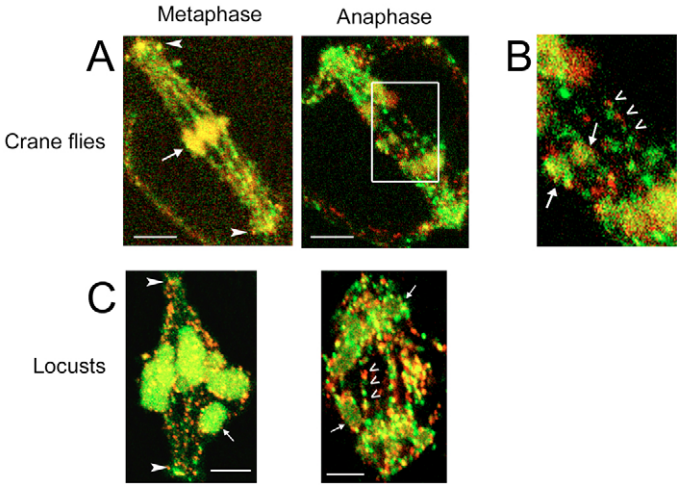

Fig. 8. Distribution of anti-KZ antibody compared with myosin distribution in insect spermatocytes. (A) Merged channels of D-titin (green) and myosin (red) staining in metaphase (left panel) and anaphase (right panel) crane-fly spermatocytes (*Z*-series), showing their co-localization (yellow-orange) in the chromosomes (arrow), at the poles (arrowheads) and along the spindle fibers. (B) Enlarged detail of the boxed region in A showing the side-by-side distribution of D-titin (green) and myosin (red) in the interzone along the connections between separating half-bivalents (open arrowheads). Arrows indicate the two sex chromosomes. (C) Merged channels of D-titin (green) and myosin (red) staining in metaphase (left panel) and anaphase (right panel) locust spermatocytes, showing their co-localization (yellow-orange) at the poles (arrowheads) and along the spindle fibers. The arrow in the left panel indicates the sex chromosome and the arrows in the right panel indicate two autosomal half bivalents. Open arrowheads indicate side-by-side distribution of D-titin and myosin staining in the interzone along the connections between separating half-bivalents. Bars, 5 μm.

Matrix protein distribution in insect spermatocytes

A putative contractile or elastic spindle matrix may anchor kinetochore fibers and exert force on them (Pickett-Heaps et al., 1982; Pickett-Heaps et al., 1984; Pickett-Heaps et al., 1996; Pickett-Heaps et al., 1997; Scholey et al., 2001; Tsai et al., 2006). Since titin has elastic properties, it may impart 'elasticity' to the spindle matrix. Thus, we co-stained cells for D-titin and skeletor, D-titin and megator, and D-titin and chromator, the three proteins being considered part of the macromolecular complex that forms the spindle matrix (Walker et al., 2000; Qi et al., 2004; Rath et al., 2004). Skeletor staining in crane-fly spermatocytes has been described previously using a different antibody (Silverman-Gavrila and Forer, 2003); we describe our skeletor staining results as well, to provide supplementary details.

We stained locust and crane-fly spermatocytes with 1A1, a monoclonal antibody against *Drosophila* skeletor (Fig. 10). In prophase of both cell types (Fig. 10A,F), skeletor antibodies

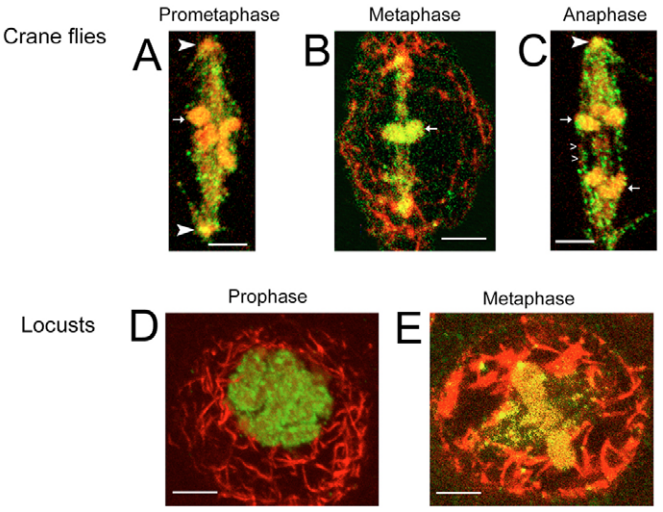

Fig. 9. Distribution of anti-KZ antibody (green) vs actin distribution (red) in insect spermatocytes. (A-C) Merged channels of D-titin and actin staining in prometaphase (A), metaphase (B) and anaphase (C) crane-fly spermatocytes (*Z*-series), showing their co-localization (yellow-orange) in the chromosomes (arrows), at the poles (arrowheads) and along the spindle fibers. (D,E) Merged channels of D-titin and actin staining in prophase (A) and metaphase (B) locust spermatocytes (*Z*-series), showing their co-localization (yellow-orange) in the chromosomes (arrow) and along the spindle fibers. Bars, 5 μm.

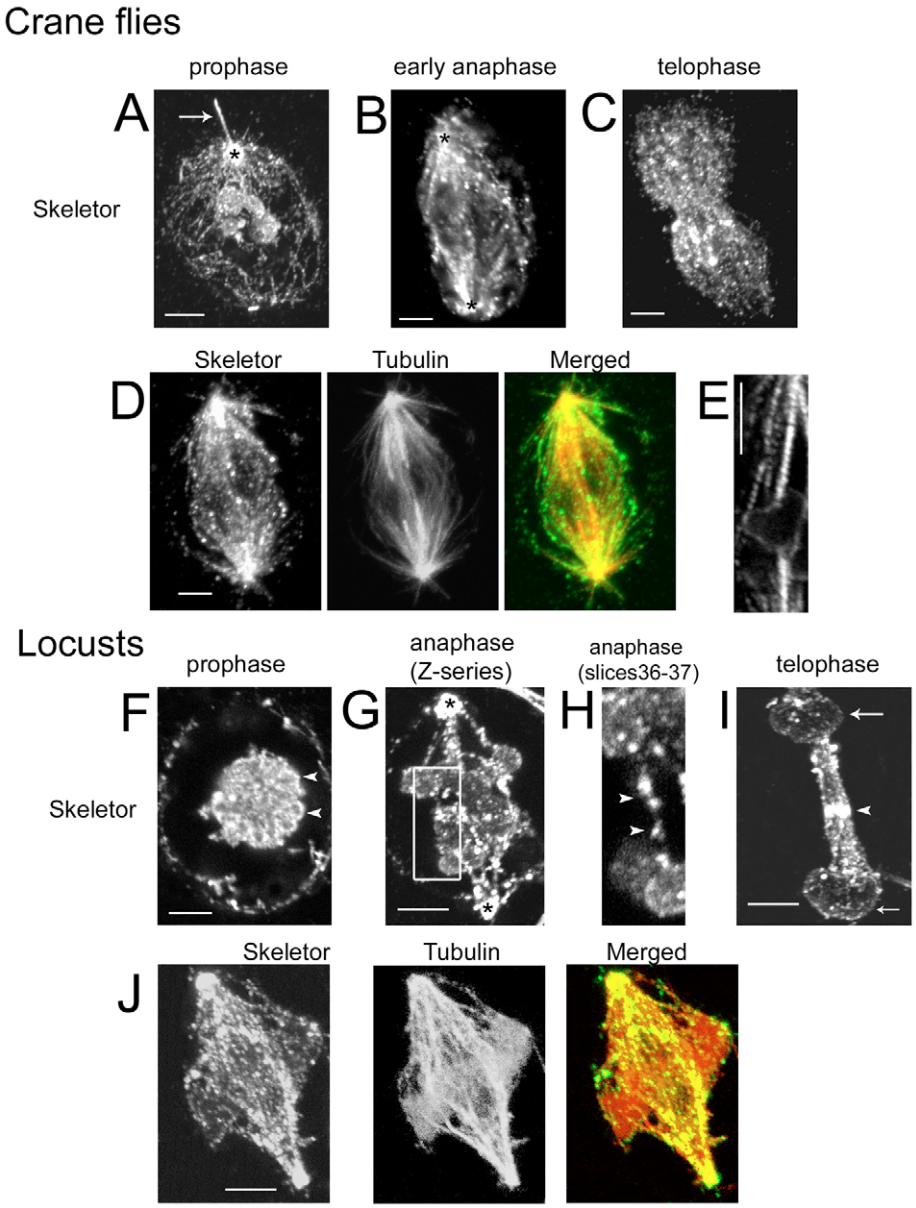

Fig. 10. Skeletor distribution in crane-fly and locust spermatocytes. (A) A prophase cell illustrating staining of chromosomes, the cell cortex, the asters, the polar flagella (arrow indicates one flagellum) and the poles (asterisk indicates one pole). (B) An early anaphase cell, illustrating staining along the kinetochore and non-kinetochore spindle fibers, defining the spindle area. Asterisks indicate the two poles. (C) A telophase/cytokinesis cell illustrating staining of the mid-body region. (D) A prometaphase cell stained for skeletor (green) and tubulin (red). Skeletor and tubulin co-localize (yellow-orange) mainly along kinetochore spindle fibers and at the poles. (E) Enlarged detail of a kinetochore spindle fiber and a bivalent at metaphase (slice 24 of the same cell depicted in Fig. 12), showing the beaded distribution of skeletor along these spindle fibers and around the chromosomes. (F) A prophase locust spermatocyte illustrating skeletor staining of the chromosomes, their periphery (arrowheads) and the cell cortex. (G) An anaphase locust spermatocyte. Skeletor is seen as punctate regions in the chromosomes, along the kinetochore spindle fibers, along the interzone connections between separating half-bivalents, and in high concentration at the poles. (H) Enlarged detail of two consecutives confocal slices (merged) of the same cell as in G, illustrating the interzone connections (arrowheads) between separating half-bivalents. (I) A telophase cell. Skeletor is present in high concentration in the mid-body, in the contractile ring (arrowhead) and in the newly formed nuclear membrane (arrows). (J) Metaphase locust spermatocyte double stained for skeletor (green) and tubulin (red). Skeletor and tubulin co-localize (yellow-orange) mainly along kinetochore spindle fibers and at the poles, similar to the pattern observed in crane-fly spermatocytes. Bars, 5 μm.

stained mainly the chromosomes and around them (Fig. 10F, arrowhead) and, to a lesser extent, the cell cortex (Fig. 10A,F). In crane-fly spermatocytes, the anti-skeletor antibodies also stained the nuclear membrane (data not shown), the asters, the polar flagella (Fig. 10A, arrow), the poles (Fig. 10A,B asterisks), and various structures in the cytoplasm (Fig. 10A). During prometaphase and metaphase, skeletor antibodies stained the spindle (where skeletor co-localized with tubulin) (Fig. 10D,J) and the poles. In individual optical sections of the spindle, skeletor had a dotted appearance, with dots distributed in high density almost uniformly along the spindle microtubules, like beads on a string (Fig. 10E). Skeletor was also distributed in puncta between spindle microtubules. When individual images from a confocal series were superposed (as a *z*-series), skeletor appeared as an almost continuous filament (Fig. 10D,J). In metaphase, more skeletor staining was apparent along the kinetochore fibers than along the non-kinetochore fibers (Fig. 10E). By anaphase, skeletor staining was mostly along the fibers (kinetochore, non-kinetochore and sex chromosome spindle fibers), and at the poles (Fig. 10B,G asterisks), but also was seen in the interzone, between the separating half bivalents (Fig. 10H, arrowheads). During telophase/cytokinesis, skeletor staining was found in the mid-body (Fig. 10C,I), in the sex chromosomes and their fibers (data not shown), and in the contractile ring [mainly in locusts (Fig. 10I, arrowhead)], with little staining in the newly formed nuclei.

We stained crane-fly and locust spermatocytes with 12F10, an antibody against megator and with 6H11, an antibody against chromator. Megator is an essential coiled-coil protein that localizes to the spindle matrix in mitotic *Drosophila* cells (Qi et al., 2004), whereas chromator is a *Drosophila* chromodomain protein that interacts directly with skeletor (Rath et al., 2004). Both of these proteins are present in crane-fly and locust spermatocytes, where they have a similar distribution. Megator and chromator have a dotted appearance;

they do not form filaments, but they are closely associated with microtubules, during all phases of division. Megator forms slightly larger dots (Fig. 11B), whereas chromator has a 'fine sand' appearance (Fig. 11E insert). During prophase of crane-fly spermatocytes, they are present mostly in the chromosomes, in the nuclear membrane and in the cytoplasm (Fig. 11A,D), where they associate with the network of microtubules. In prophase of locust spermatocytes, megator distribution is similar to that described for crane-flies (Fig. 11G), but chromator localizes only to the chromosomes (Fig. 11J). In metaphase and anaphase, they are present in the spindle and along all microtubules (kinetochore, polar, astral microtubules) (Fig. 11B,E); megator staining also is present between and outside the spindle fibers (Fig. 11B). Megator and chromator have a similar distribution in metaphase and anaphase locust spermatocytes spindles (Fig. 11H,K), as they have in crane-fly spermatocyte spindles, but they also are found in the locust chromosomes, whereas neither one is present in crane-fly chromosomes. During telophase/cytokinesis, these molecules are present in the midbody, but not in the contractile ring (Fig. 11C,F,I), except for chromator, which in locust spermatocytes is very weak in the midbody, but is present in the contractile ring (Fig. 11L). The antibodies against megator and chromator also stain the newly formed nuclei, with higher intensity in locust spermatocytes compared with crane-fly spermatocytes.

D-titin distribution compared with matrix protein distribution

When locust and crane-fly spermatocytes were double stained for skeletor and D-titin (stained with anti-KZ), the two proteins co-localized at the poles (Fig. 12A, asterisks; data not shown for locust), along the spindle microtubules (Fig. 12B slice 25 arrowheads), in the 'envelope' around the chromosomes (Fig. 12A, arrow) and in the interzone (data not shown), in that almost all dots appear yellow/orange in merged images.

Double staining of locust and crane-fly spermatocytes for D-titin and megator or for D-titin and chromator, indicates that these proteins also co-localize along spindle fibers and at the poles (data not shown). The tight co-localization of D-titin and skeletor, megator or chromator suggests that these proteins might interact in a spindle matrix, perhaps involved in spindle rigidity, force production and/or tension generation during anaphase.

Discussion

In this study we have shown that a titin-like protein is present

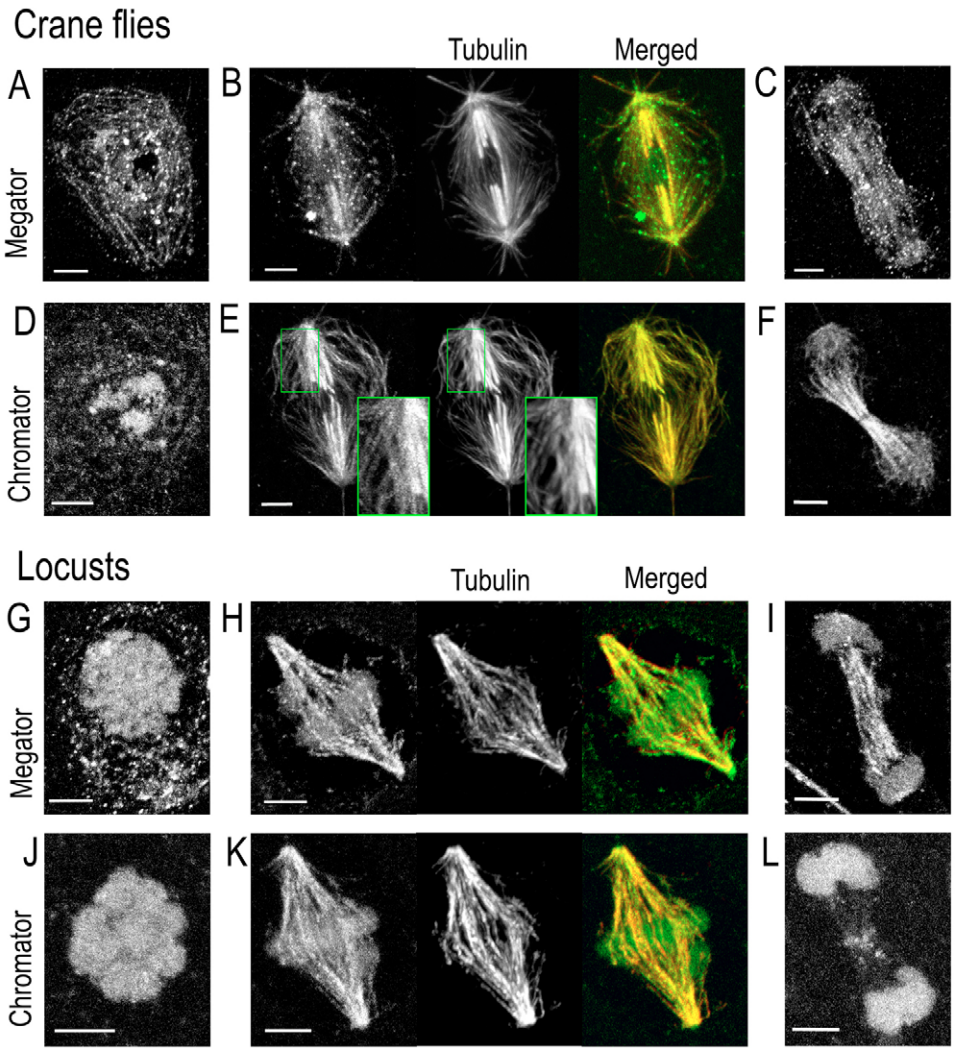

Fig. 11. Megator and chromator distribution in crane-fly and locust spermatocytes. (A,D,G,J) Prophase spermatocytes illustrating megator (A,G) and chromator (D,J) staining of chromosomes. (B,E,H,K) Metaphase spermatocytes double stained for megator and tubulin (B,H) and for chromator and tubulin (E,K), illustrating spindle fiber staining. Left panels in B,E,H,K show megator or chromator staining, middle panels show tubulin staining and right panels show the merged image of the two channels (green, megator or chromator; red, tubulin; yellow-orange, co-localization). Inserts in E are enlarged images of the boxed regions and illustrate differences between chromator and tubulin: chromator has a fine granular appearance along spindle fibers, whereas tubulin has a filamentous appearance. (C,F,I,L) Telophase/cytokinesis spermatocytes illustrating megator (C,I) and chromator (F,L) staining of midbody, newly formed nuclei and contractile ring (L). Bars, 5 μm.

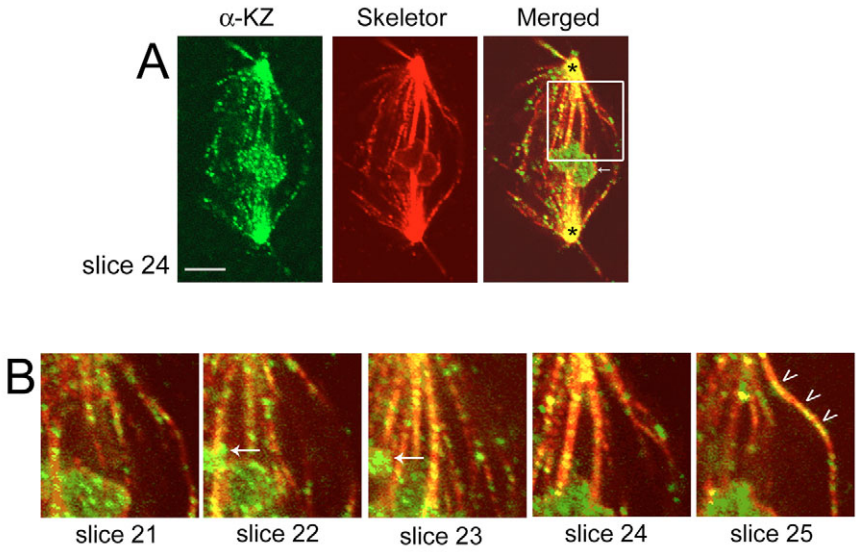

Fig. 12. A prometaphase crane-fly spermatocyte stained for D-titin with anti-KZ antibody (green) and for skeletor (red). (A) D-titin and skeletor co-localize (yellow-orange) along kinetochore and non-kinetochore spindle fibers and at the poles (asterisks). Arrow indicates one autosomal bivalent. (B) Enlarged details of the boxed region in A showing D-titin vs skeletor distribution along spindle fibers in five consecutives slices to illustrate their spatial localization in the *Z*-axis. Arrows indicate one sex chromosome. Open arrowheads indicate D-titin vs skeletor localization along non-kinetochore microtubules. Bar, 5 μm.

in locust and crane-fly spermatocytes, associated with the chromosomes, the spindle in general, kinetochore microtubules, non-kinetochore microtubules, spindle poles, and extending as apparent connections between separating partner half-bivalents, based on staining with three antibodies for D-titin. Several lines of evidence attest to the validity that we identified a titin-like protein. Firstly, the three antibodies we used recognize D-titin, as indicated by the fact that all three antibodies, each of which was produced against a different, spatially separate fragment of the protein, stained the same cell components in *Drosophila* embryos, in crane-fly spermatocytes and in locust spermatocytes. The co-staining of the same components would be difficult to explain under any hypothesis other than that the three antibodies stain the same protein: it is extremely unlikely, for example, that three unrelated proteins would have identical localization patterns throughout all stages of cell division. Since the antibodies were synthesized against epitopes from three distinct fragments of D-titin, the most likely possibility is that a titin-like protein is recognized by each of the antibodies. Data from the western blot analysis support this conclusion, illustrating that all three anti-D-titin antibodies reacted with high molecular mass proteins from insect muscle, which appeared to be the same as the insect 'mini-titin' isolated by Nave and Weber (Nave and Weber, 1990); these data indicate that the three antibodies we used indeed recognize a titin-like protein in insect muscle. Further, staining of glycerinated myofibrils results in prominent staining at the Z-lines of a protein distinct from actin or myosin, similar to staining of mini-titin (Nave and Weber, 1990). We found that this protein changes its distribution when the sarcomeres change length, as expected of a titin-like protein. Mass spectrometry analysis confirmed that high molecular mass bands from muscle contain titin. Thus, we are confident that the described staining patterns in crane-fly and locust spermatocytes are indeed due to D-titin.

Next, we did a variety of controls for the staining procedures: we omitted the primary antibodies; we stained for one protein at a time; we used different secondary antibodies with the same primary antibody; we changed the order of the double staining; we used secondary antibodies with different fluorochromes; and we used a variety of fixation procedures. Results from these control experiments indicate that the staining is due to the primary antibody and is not specific to any single fixation or lysis procedure. Thus, we are confident that the described staining patterns represent non-perturbed patterns of D-titin localization, patterns consistent with staining observed in *C. elegans* spindles (Zastrow et al., 2006) and in mammalian spindles (Wernyj et al., 2001). Whereas Machado et al. (Machado et al., 1998) did not report staining of spindle fibers in *Drosophila* or mammalian cells with anti-KZ, the same anti-KZ antibody in the present study did stain spindle fibers. The difference in staining might be explained because Machado and colleagues included RNase in their staining protocol. As we have shown here, RNase treatment causes a drastic increase in chromosome staining with anti-KZ antibody (Fig. 7F), making it difficult to detect the spindle staining. We do not know why this change occurs, but it is possible that RNA has a structural role in the spindle (Blower et al., 2005) and after RNase treatment the titin epitopes that recognize the anti-KZ antibodies might become unavailable (masked) by changes in the spindle fiber, whereas the epitopes for anti-56 are still exposed and the antibodies can bind to titin regions corresponding to the anti-56 domain.

Although we have no functional data on the role of spindle D-titin, several aspects of spindle physiology are congruent with known roles of D-titin. For one, a putative spindle matrix might provide flexibility and elasticity as an underlying component of spindles, and the matrix might even be involved in force production (Forer et al., 2003; Fabian and Forer, 2005). We used the term 'putative' because there has been no definitive molecular or morphological description of a matrix, except that the *Drosophila* proteins skeletor, megator and chromator would seem to be components of (or at least markers of) such a matrix. Skeletor, megator and chromator staining reveals the expected morphology, and skeletor and megator distribution maintain a spindle shape even after spindle microtubules have been depolymerized (Johansen, 1996; Johansen et al., 1996; Walker et al., 2000; Qi et al., 2004; Rath

et al., 2004). Since titin has a major role in the elasticity of skeletal and cardiac muscle, and since it is closely associated with skeletor in the spindle, it is reasonable to think that skeletor and D-titin function physiologically as part of a spindle matrix. Spindle actin and myosin are closely associated with D-titin and skeletor, so they, too, might be part of such a matrix. Our data suggest that the interactions among these proteins (D-titin, skeletor, myosin and actin) and between these proteins and the spindle microtubules change during the course of cell division, as illustrated in the cartoon (Fig. 13). Skeletor, for example, is present along the spindle fibers and in between them (the 'matrix') throughout the course of division, but it accumulates progressively in the kinetochore microtubule bundles as division proceeds towards anaphase. D-titin in chromosomes is present in high concentration in prophase but by metaphase and anaphase, the staining of the chromosomes is somewhat reduced, as determined by comparing their staining intensities with that of muscle fibers in the same preparations. In prophase, D-titin is present in the cytoplasmic asters. After nuclear membrane breakdown, as the development of the spindle proceeds towards anaphase, D-titin becomes increasingly concentrated at the poles and along kinetochore fibers with the staining along the kinetochore fibers eventually being as high as 80-85% the levels of staining observed in muscle fibers. Thus, we might speculate that the interactions among these proteins develop and continue throughout prometaphase to culminate in a 'mature' matrix by metaphase.

Another potential role for D-titin in spindles may be as part of the elastic 'tethers' extending between arms of separating half-bivalents in crane-fly spermatocytes. Evidence for these tethers comes from experiments showing that laser-severed chromosome arms or entire chromosomes move backwards across the equator (Ilagan et al., 1997; LaFountain et al., 2002; Wong and Forer, 2004). D-titin extends between the arms of separating half-bivalents (Fig. 6A insert and Fig. 8B), so it is reasonable to suggest that the tethers contain D-titin, and that D-titin is responsible for tether elasticity, at least in part.

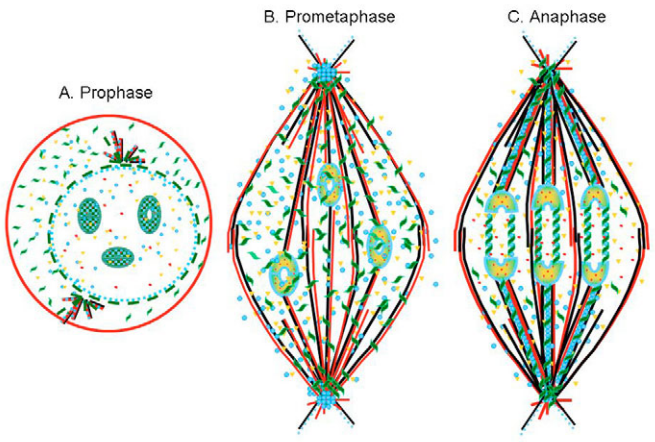

Fig. 13. Model illustrating the changing distributions of the proteins studied. D-titin (green), skeletor (blue), actin (red), myosin (yellow) and tubulin (black) in prophase (A), prometaphase (B) and in anaphase (C). Three chromosome bivalents (A,B) or three separating pairs of half-bivalents (C) are illustrated. The changing distribution patterns are described in detail in the text.

Another possible role is suggested by recent experiments in which titin modulates the velocity of actin filaments that slide along an HMM-coated surface (Nagy et al., 2004), titin-actin interactions acting as a 'viscous bumper mechanism' to slow the movements. One could envisage a similar effect on the velocity of chromosome movement because titin can interact with microtubules in addition to muscle proteins (Pizon et al., 2002).

The identification of D-titin in spindles, together with other muscle proteins, actin, myosin (Forer et al., 2003) and zyxin (Hirota et al., 2000), suggest that these proteins indeed function during mitosis, perhaps in a spindle matrix and in producing forces for chromosome movement. If we knew the arrangements (and polarities) of these proteins in the spindle, we might better understand their function. With respect to D-titin, following several markers could, in theory, give information about how the molecules are arranged; since D-titin is so large, double staining with different antibodies could result in resolvable separation for epitopes reasonably far apart on the molecule. We did indeed find separate dots after staining with the three different antibodies. Because the staining is punctate, and the molecules are arranged in three dimensions and not just the two observed in the image, we cannot be certain of the arrangement of the individual D-titin molecules. Nonetheless, if it is true that two D-titin epitopes are 2 μm apart along the length of the kinetochore microtubules, but only 0.2 μm apart at an oblique angle, as seen in double stained images (Fig. 7), this would suggest that the individual D-titin molecules may be arranged obliquely to the kinetochore microtubules rather than along them.

The presence of D-titin in prophase nuclear membranes (Fig. 4A, arrows) and in nascent membranes formed around the daughter nuclei in telophase (Fig. 6G, arrows), is consistent with the finding that D-titin is associated with and binds to lamins, as found in *C. elegans* by Zastrow et al. (Zastrow et al., 2006).

Materials and Methods

Antibody production and staining of *Drosophila* embryos

Production of the rat antiserum designated anti-KZ was described previously (Machado et al., 1998). To produce the anti-52 and anti-56 antisera, fragments from cDNA clones LP06352 and CK00556 were amplified by PCR, subcloned into the pTRCHisA expression vector (Invitrogen, Carlsbad, CA) and transformed into BL21 (DE3) cells. Protein was purified from inclusion bodies 3-6 hours after induction with 0.1 mM IPTG (Isopropyl β-D-1-thiogalactopyranoside). Rabbit polyclonal antiserum was raised (Covance, Denver, PA) against 2.5 mg of renatured inclusion body protein from the LP06352 clone (anti-52) and guinea pig polyclonal antiserum was raised against 1.2 mg of renatured inclusion body protein from the CK00556 clone (anti-56). Staining of *Drosophila* embryos with each of the anti-titin polyclonal antisera were performed as described (Reuter et al., 1990), using anti-52 antiserum at a dilution of 1:5000, anti-56 antiserum at a dilution of 1:500 and anti-KZ at a dilution of 1:5000.

Staining and confocal microscopy of spermatocytes

We studied crane-fly spermatocytes because of the wealth of previous data on their cytology and chromosome behavior. We also studied locust spermatocytes to see whether the results are restricted to crane-fly spermatocytes (see Fabian and Forer, 2007).

Testes from fourth-instar crane-fly larvae or fifth-instar locusts were removed under Halocarbon oil and rinsed for several minutes with insect Ringer's solution (0.13 M NaCl, 5 mM KCl, 1 mM $CaCl_2$, 3-5 mM phosphate buffer, final pH 6.8-6.9) or with Belar's solution (Belar, 1929), respectively. Crane-fly testes (or lobes of locust testes) were placed in 3-4 μl fibrinogen solution (10 mg/ml), cells were spread and 2.5 μl thrombin was added to form a fibrin clot, after which the cells were perfused with Ringer's solution or Belar's solution (Forer and Pickett-Heaps, 1998; Forer and Pickett-Heaps, 2005). In some preparations, the fibrinogen solution contained muscle fibers freshly removed from the thorax of a living crane-fly; the

myofibers were macerated in insect Ringer's solution and fibrinogen was dissolved in the solution. Spermatocytes were then spread in this solution as described above.

Preparations of living cells were lysed for at least 15 minutes with regular lysis buffer (100 mM PIPES, 10 mM EGTA, 5 mM $MgSO_4$, pH 6.9; 1% NP40 and 5% DMSO), fixed for 3-5 minutes in 0.25% glutaraldehyde in phosphate buffered saline (PBS), then treated for 15 minutes with sodium borohydride (1 mg/ml) to neutralize free aldehyde groups, and stored in 1:1 (v/v) PBS/glycerol, at 4°C. In addition to this (our 'regular') protocol, we also tried various other protocols: we replaced NP40 with 1.5% CHAPS (Toronto Research Chemicals Inc.), or we added 1% Triton X-100 to our regular lysis buffer, or reduced the glutaraldehyde concentration to 0.1%, or reduced the fixation time to 1-2 minutes, or we performed lysis and fixation as one step by adding 0.1% glutaraldehyde to the lysis buffer (containing either NP40 or CHAPS), or we performed the fixation as the first step (20 seconds to 1 minute) and then lysed the cells, or we used Bouin's fluid (0.66% picric acid, 9.5% formalin, 4.7% acetic acid) (Walker et al., 2000) as a fixative, either mixed with 1% NP40 or added after regular lysis.

The staining protocol used for preparations of spermatocytes was modified from that of Czaban and Forer (Czaban and Forer, 1992) and Wilson et al. (Wilson et al., 1994). Before staining, coverslips were rinsed in PBS with 0.1% Triton X-100 to ensure uniform spreading of the antibody solution. The incubation time for each antibody and for phalloidin was 45 minutes at room temperature, and the preparations were kept in the dark, to prevent light inactivation of the fluorochromes. The primary antibodies were diluted in PBS and used as follows: rat KZ anti D-titin (anti-KZ) at 1:500 (Machado et al., 1998); rabbit LP06352 anti D-titin (anti-52) at 1:500; guinea pig CK00556 anti D-titin (anti-56) at 1:500; mouse α-tubulin IgG (Cedarlane) at 1:500; Alexa phalloidin (Molecular Probes) against filamentous actin at 2.2 μM; mouse IgM My-21 (Sigma) against myosin II regulatory light chain at 1:200; mouse IgM mAb1A1 against skeletor (Walker et al., 2000) at 1:100; mouse 6H11 against chromator at 1:100 (Rath et al., 2004) and mouse 12F10 against megator at 1:100 (Qi et al., 2004). All the secondary antibodies were Alexa fluorochromes (Molecular Probes). In a few specific experiments, we added 100 μg/ml RNase I (Sigma) to the solutions containing the primary and secondary antibodies, as described in Machado et al. (Machado et al., 1998). After staining, the samples were mounted in Mowiol containing paraphenylene diamine as an antifading agent. Cells were examined with a Bio-Rad MRC 600 or an Olympus Fluoview 300 confocal microscope. The images were collected with COMOS (Bio-Rad) or Fluoview (Olympus) software, and were processed further using Confocal Assistant (public domain software available at ftp://ftp.genetics.bio-rad.com/Public/confocal/cas), Image J (public domain software available at http://rsb.info.nih.gov/ij/) and Adobe Photoshop. Illustrations presented in this paper were obtained using Adobe Photoshop and were adjusted for image presentation only (brightness, contrast, pseudocoloring). Unless otherwise indicated in the figure legends, all illustrations are of cells prepared using our regular lysis/fixation protocol, without RNase, and are *Z*-projections of several sections.

Myofibril preparations for immunofluorescence

The thorax of crane-fly adults was dissected under Ringer's solution and the muscle fibers were stretched with forceps and immersed in glycerol/standard salts 1:1 (v/v) in a test tube. Standard salts solution is 0.05 M KCl, 1 mM $MgCl_2$, 5 mM phosphate buffer, pH 6.8. After 48 hours, the myofibrils were squished up and down using a Pasteur pipette, vigorously vortexed and then the solution was centrifuged for 10 minutes at 13,000 ***g*** to remove pieces of chitinous thorax. The supernatant contained myofibrils and was kept at 4°C until used in preparations. To make preparations, a 0.5 ml aliquot of myofibrils in glycerol/standard salts was diluted in 5 ml standard salts, centrifuged at 13,400 ***g***, in an MSE GT-2 centrifuge, for 10 minutes and the pellet suspended in 0.7 ml standard salts solution. Fibrinogen solution was made by adding 7 mg fibrinogen to the 0.7 ml myofibril suspension. To make a fibrin clot preparation, 2.5-5 μl of fibrinogen-myofibril solution were spread on a coverslip and the same amount of thrombin solution was added, following the procedure described for crane-fly and locust spermatocytes. The myofibril preparations were then lysed, fixed and stained as described in the previous section for spermatocytes.

Quantitative analysis of staining intensities

We estimated the amount of D-titin staining of spindle fibers and chromosomes in crane-fly spermatocytes. We obtained a sequence of (*Z*-series) images of stained myofibers on the same slides as the spermatocytes, using the same microscope conditions for cells and myofibers (i.e. the same gain, laser intensity, etc.) and under conditions in which neither the lower nor the upper limit of gray scale was reached. Using Image J software, lines were drawn in individual sections over regions of interest: along the stained portions of myofibers, along kinetochore spindle fibers or along chromosomes. The lines were converted to plots of gray scale versus position (along the length of each line), the lines were plotted on graphs (using commercially available SlideWrite software), and, for each line, we obtained average values for the gray scale intensities. The average intensities of myofiber staining were compared with average intensities of chromosome staining, and were compared with both average and maximum intensities of staining along kinetochore fibers. We looked at maximum staining intensities along kinetochore fibers because their anti-D-titin staining was punctate rather than continuous.

Western blots

Insect muscle samples for immunoblotting were placed in insect Ringer's solution containing protease inhibitors (10 μg/ml PMSF, 10 μg/ml E64 and 1:100 Bioshop protease inhibitors cocktail). The samples were homogenized in sample buffer [8 M urea, 2 M thiourea, 75 mM dithiothreitol, 3% SDS (w/v), 0.05 M Tris-HCl pH 6.8, 0.03% Bromophenol Blue, Bioshop protease inhibitor cocktail 1:50], heated at 60°C for 10 minutes to solubilize titin without degrading it (Warren et al., 2003) and centrifuged at 13,400 ***g*** in a MSE GT-2 centrifuge, for 15 minutes. The supernatant was removed, snap frozen in a mix of ethanol and dry ice, and stored at –80°C. Proteins from rat soleus muscle, prepared as described in Warren et al. (Warren et al., 2003), were used as molecular weight markers.

The protein extracts were separated on 1% w/v agarose gels (10 cm high) using a Bio-Rad Mini PROTEAN II system (Laemmli, 1970), following a protocol modified from Warren et al. (Warren et al., 2003). A 0.75 cm high acrylamide plug (12% acrylamide, 10% glycerol, 0.5 M Tris-HCl pH 9.3, 0.028% freshly prepared ammonium persulfate, 0.152% TEMED) was poured between the glass plates; after it hardened, the agarose gel was poured on top. The resolving gel contained 1% w/v SeaKem Gold agarose (Cambrex), 30% glycerol, 50 mM Tris base, 0.384 M glycine and 0.1% SDS. The electrophoresis buffer had the same composition in the lower and in the upper chambers (50 mM Tris base, 0.384 M glycine, 0.1% SDS, 10 mM mercaptoethanol). Gels were run at 20 mA constant current for about 2 hours, at 8°C, until the front reached the bottom of the agarose gel.

Some of the agarose gels (or several lanes only) were stained overnight with 0.05% Coomassie Brilliant Blue R-250, at room temperature. For other gels, the proteins were electroblotted onto PVDF membrane (BioRad 0.2 μm pore) at 20 V for 2 hours in transfer buffer containing 10 mM 3-[cyclohexylamino]-1-propanesulfonic acid (CAPS) buffer pH 11, 0.1% SDS, 10 mM mercaptoethanol and 10% methanol. We reduced the voltage and the time of the transfer from those indicated by Warren et al. (Warren et al., 2003) because the proteins passed through the membrane, not only in the direction of the anode, but in the opposite direction, as well. The membrane was blocked in 5% Blotto in TBST (0.05% w/v Tween-20 in TBS) for 2 hours, rinsed three times for 10 seconds with ddH_2O, twice for 5 minutes each with TBST, and incubated with various primary antibodies overnight, at 8°C [anti-KZ (rat) 1:500; anti-52 (rabbit) 1:500; anti-56 (guinea pig) 1:500]. The immunoblots were washed six times for 5 minutes each with TBST, and incubated for 2 hours at room temperature with the appropriate secondary antibody [HRP-conjugated 1:5000 Goat anti-rat (Sigma), 1:2000 Goat anti-rabbit (Bio-Rad), or 1:5000 Rabbit anti-guinea pig (Sigma)]. Membranes were washed five times for 5 minutes each with TBST and once for 10 minutes with TBS and the signals were detected by enhanced chemiluminescence (ECL) (Amersham Biosciences). Several exposure times were used, but the developing and fixing times were always 1 minute each. After exposure, the antibodies were stripped off the membranes, leaving the antigens intact, using the protocol described by Legocki and Verma (Legocki and Verma, 1981). The stripped blots were tested for residual signal, blocked in 5% Blotto and reprobed with another anti-D-titin antibody. The negatives were scanned with an Arcus 1200 AGFA scanner and digitized using Photoshop software (Adobe).

Mass spectrometry

High molecular mass bands from the agarose gels stained with Coomassie Blue were cut with a clean razor blade and digested separately with trypsin, using an in-gel tryptic procedure (Shvechenko et al., 1996) at the Centre for research in Mass Spectrometry (York University, Toronto, Canada). The extracted tryptic peptides were dried by a speed vacuum and stored at –20°C (Jacobs et al., 2006). Samples were resuspended in 10 μl of 0.3% trifluoroacetic acid (TFA) and desalted using C_{18} Ziptips (Millipore). Samples were eluted with 1 μl of α-cyano matrix solution (10 mg/ml in 60% acetonitrite, 0.3% TFA solution) and spotted on a MALDI target plate.

Mass spectrometry analysis (MS) was performed on a QSTAR XL (AB/Sciex) instrument with a MALDI source. The most intense peaks from the MS scans were chosen for fragmentation by tandem MS (MS/MS analysis). The MS/MS scans were searched against a non-redundant NCBI database of eukaryote sequences using MASCOT (Matrix Science). The peptides matched gi/91076016 from *Tribolium castaneum* with a score of 61. This sequence, when aligned using NCBI's BLAST algorithm, matched the protein titin from various organisms, including *Drosophila*.

We thank Michael Zastrow (The Johns Hopkins University School of Medicine) for communicating his results on *C. elegans* prior to their publication. Many thanks and gratitude to Anne and Barrie Coukell (York University) and Peter Adhihetty (York University) for helping with the western blots and for many useful discussions and suggestions on gels and westerns, and for giving us the rat soleus muscle. We are grateful to Robert L. S. Perry (York University) for help and guidance with ECL, and for use of some reagents for ECL visualization of the westerns. Many thanks to Leroi DeSouza (Centre for Research in Mass Spectrometry, Toronto, Canada) for doing the MS analysis and for helpful discussions on the MS scans and their

interpretation. The work was supported in part by grants from the Canadian Natural Sciences and Engineering Council to A.F., from the March of Dimes to D.J.A. and from the National Science Foundation (MCB-0445182) to K.M.J. and by an Ontario Graduate Scholarship to L.F.

References

Belar, K. (1929). Beitrage zur Kausalanalyse der Mitose. II. Untersuchungen an den Spermatocyten von Chorthippus (Stenobothrus) lineatus Pans. *Z. Wiss. Biol. Arch. Entwicklungsmechanik* **118**, 359-484.

Blower, M. D., Nachury, M., Heald, R. and Weis, K. (2005). A Rae1-containing ribonucleoprotein complex is required for mitotic spindle assembly. *Cell* **121**, 223-234.

Czaban, B. B. and Forer, A. (1992). Rhodamine-labelled phalloidin stains components in the chromosomal spindle fibres of crane-fly spermatocytes and *Haemanthus* endosperm cells. *Biochem. Cell Biol.* **70**, 664-676.

Eilertsen, K. J. and Keller, T. C. S., III (1992). Identification and characterization of two huge protein components of the brush border cytoskeleton: evidence for a cellular isoform of titin. *J. Cell Biol.* **119**, 549-557.

Eilertsen, K. J., Kazmierski, S. T. and Keller, T. C. S., III (1994). Cellular titin localization in stress fibers and interaction with myosin II filaments in vitro. *J. Cell Biol*. **126**, 1201-1210.

Fabian, L. and Forer, A. (2005). Redundant mechanisms for anaphase chromosome movements: crane-fly spermatocyte spindles normally use actin filaments but also can function without them. *Protoplasma* **225**, 169-184.

Fabian, L. and Forer, A. (2007). Mechanisms of anaphase chromosome movements in locust spermatocytes. *Protoplasma* In press.

Fabian, L., Troscianczuk, J. and Forer, A. (2007). Calyculin A, an enhancer of myosin, speeds up anaphase chromosome movement. *Cell Chromosome* **6**, 1.

Flaherty, D. B., Gernert, K. M., Shmeleva, N., Tang, X., Mercer, K. B., Borodovsky, M. and Benian, G. M. (2002). Titins in *C. elegans* with unusual features: coiled-coil domains, novel regulation of kinase activity and two new possible elastic regions. *J. Mol. Biol*. **323**, 533-549.

Forer, A. and Pickett-Heaps, J. D. (1998). Cytochalasin D and latrunculin affect chromosome behaviour during meiosis in crane-fly spermatocytes. *Chromosome Res.* **6**, 533-549.

Forer, A. and Pickett-Heaps, J. D. (2005). Fibrin clots keep non-adhering living cells in place on glass for perfusion or fixation. *Cell Biol. Int.* **29**, 721-730.

Forer, A., Spurck, T., Pickett-Heaps, J. D. and Wilson, P. J. (2003). Structure of kinetochore fibres in crane-fly spermatocytes after irradiation with an ultraviolet microbeam: neither microtubules nor actin filaments remain in the irradiated region. *Cell Motil. Cytoskeleton* **56**, 173-192.

Furst, D., Osborn, M., Nave, R. and Weber, K. (1988). The organization of titin filaments in the half-sarcomere revealed by monoclonal antibodies in immunoelectron microscopy: a map of ten non-repetitive epitopes starting at the Z line extends close to the M line. *J. Cell Biol.* **106**, 1563-1572.

Gassner, D., Shraideh, Z. and Wohlfarth-Bottermann, K.-E. (1985). A giant titin-like protein in *Physarum polycephalum*: evidence for its candidacy as a major component of an elastic cytoskeletal superthin filament lattice. *Eur. J. Cell Biol*. **37**, 44-62.

Granzier, H. L. and Irving, T. C. (1995). Passive tension in cardiac muscle: contribution of collagen, titin, microtubules, and intermediate filaments. *Biophys. J*. **68**, 1027-1044.

Gregorio, C. C., Trombitas, K., Centner, T., Kolmerer, B., Stier, G., Kunke, K., Suzuki, K., Obermayr, F. and Herrmann, B. (1998). The NH2 terminus of titin spans the Z-disk: its interaction with a novel 19-kD ligand (t-cap) is required for sarcomeric integrity. *J. Cell Biol.* **143**, 1013-1027.

Hirota, T., Morisaki, T., Nishiyama, Y., Marumoto, T., Tada, K., Hara, T., Masuko, N., Inagaki, M., Hatakeyama, K. and Saya, H. (2000). Zyxin, a regulator of actin filament assembly, targets the mitotic apparatus by interacting with h-warts/LATS1 tumor suppressor. *J. Cell Biol.* **149**, 1073-1086.

Hooper, S. L. and Thuma, J. B. (2005). Invertebrate muscles: muscle specific genes and proteins. *Physiol. Rev*. **85**, 1001-1060.

Horowits, R., Maruyama, K. and Podolsky, R. J. (1989). Elastic behaviour of connectin filaments during thick filament movement in activated skeletal muscle. *J. Cell Biol*. **109**, 2169-2176.

Houchmandzadeh, B. and Dimitrov, S. (1999). Elasticity measurements show the existence of thin rigid cores inside mitotic chromosomes. *J. Cell Biol.* **145**, 215-223.

Ilagan, A. B., Forer, A. and Spurck, T. (1997). Backward chromosome movement in anaphase, after irradiation of kinetochores or kinetochore fibres. *Protoplasma* **98**, 20-26.

Itoh, Y., Suzuki, T., Kimura, S., Ohashi, K., Higuchi, H., Sawada, H., Shimizu, T., Shibata, M. and Maruyama, K. (1988). Extensible and less-extensible domains of connectin filaments in stretched vertebrate skeletal muscle sarcomeres as detected by immunofluorescence and immunoelectron microscopy using monoclonal antibodies. *J. Biochem*. **104**, 504-508.

Jacobs, M. E., DeSouza, L. V., Samaranayake, H., Pearlman, R. E., Siu, K. W. M. and Klobutcher, A. (2006). The *Tetrahymena thermophila* phagosome proteome. *Eukaryot. Cell* **5**, 1990-2000.

Johansen, K. M. (1996). Dynamic remodeling of nuclear architecture during the cell cycle. *J. Cell. Biochem.* **60**, 289-296.

Johansen, K. M., Johansen, J., Baek, K.-H. and Jin, Y. (1996). Remodeling of nuclear architecture during the cell cycle in *Drosophila* embryos. *J. Cell. Biochem.* **63**, 268-279.

Labeit, D., Watanabe, K., Witt, C., Fujita, H., Wu, Y., Lahmers, S., Funck, T., Labeit, S. and Granzier, H. (2003). Calcium-dependent molecular spring elements in the giant protein titin. *Proc. Natl. Acad. Sci. USA* **100**, 13716-13721.

Laemmli, V. K. (1970). Cleavage of structural proteins during assembly of the head of bacteriophage T4. *Nature* **227**, 680-685.

LaFountain, J. R., Oldenbourgh, R., Cole, R. W. and Rieder, C. L. (2001). Microtubule flux mediates poleward motion of acentric chromosome fragments during meiosis in insect spermatocytes. *Mol. Biol. Cell* **12**, 4054-4065.

LaFountain, J. R., Cole, R. W. and Rieder, C. L. (2002). Partner telomeres during anaphase in crane-fly spermatocytes are connected by an elastic tether that exerts a backward force and resists poleward movement. *J. Cell Sci.* **115**, 1541-1549.

Lange, S., Ehler, E. and Gautel, M. (2006). From A to Z and back? Multicompartment proteins in the sarcomere. *Trends Cell Biol*. **16**, 11-18.

Legocki, R. P. and Verma, D. P. S. (1981). Multiple immunoreplica technique: screening for specific proteins with a series of different antibodies using one acrylamide gel. *Analyt. Biochem.* **111**, 385-392.

Linke, W. A., Rudy, D. E., Centner, T., Gautel, M., Witt, C., Labeit, S. and Gregorio, C. C. (1999). I-band titin in cardiac muscle is a three-element molecular spring and is critical for maintaining thin filament structure. *J. Cell Biol.* **146**, 631-644.

Machado, C. and Andrew, D. J. (2000a). D-Titin: a giant protein with dual roles in chromosomes and muscles. *J. Cell Biol.* **151**, 639-651.

Machado, C. and Andrew, D. J. (2000b). Titin as a chromosomal protein. In *Elastic Filaments of the Cell* (ed. H. L. Granzier and G. H. Pollack), pp. 221-236. New York: Kluwer Academic/Plenum Publishers.

Machado, C., Sunkel, C. E. and Andrew, D. J. (1998). Human antibodies reveal titin as a chromosomal protein. *J. Cell Biol.* **141**, 321-333.

Maruyama, K., Murakami, F. and Ohashi, K. (1977). Connectin, an elastic protein of muscle. Comparative biochemistry. *J. Biochem.* **82**, 339-345.

Miller, M. K., Granzier, H., Ehler, E. and Gregorio, C. C. (2004). The sensitive giant: the role of titin-based stretch sensing complexes in the heart. *Trends Cell Biol.* **14**, 112-126.

Minajeva, A., Kulke, M., Fernandez, J. M. and Linke, W. A. (2001). Unfolding of titin domains explains the viscoelastic behavior of skeletal myofibrils. *Biophys. J*. **80**, 1442-1451.

Nagy, A., Cacciafesta, P., Grama, L., Kengyel, A., Málnási-Csizmadia, A. and Kellermayer, M. S. Z. (2004). Differential actin binding along the PEVK domain of skeletal muscle titin. *J. Cell Sci.* **117**, 5781-5789.

Nave, R. and Weber, K. (1990). A myofibrillar protein of insect muscle related to vertebrate titin connects Z band and A band: purification and molecular characterization of invertebrate mini-titin. *J. Cell Sci.* **95**, 535-544.

Neagoe, C., Opitz, C. A., Makarenko, I. and Linke, W. A. (2003). Gigantic variety: expression patterns of titin isoforms in striated muscles and consequences for myofibrillar passive stiffness. *J. Muscle Res. Cell Motil.* **24**, 175-189.

Obermann, V. M. J., Gautel, M., Weber, K. and Furst, D. O. (1997). Molecular structure of the sarcomeric M-band: mapping of titin and myosin binding domains in myomesin and the identification of a potential regulatory phosphorilation site in myomesin. *EMBO J*. **16**, 211-220.

Pickett-Heaps, J. D., Tippit, D. H. and Porter, K. R. (1982). Rethinking mitosis. *Cell* **29**, 729-744.

Pickett-Heaps, J. D., Spurck, T. and Tippit, D. (1984). Chromosome motion and the spindle matrix. *J. Cell Biol.* **99**, 137s-143s.

Pickett-Heaps, J. D., Forer, A. and Spurck, T. (1996). Rethinking anaphase: where "Pac-Man" fails and why a role for the spindle matrix is likely. *Protoplasma* **192**, 1-10.

Pickett-Heaps, J. D., Forer, A. and Spurck, T. (1997). Traction fibre: toward a "tensegral" model of the spindle. *Cell Motil. Cytoskeleton* **37**, 1-6.

Pizon, V., Iakovenko, A., van der Ven, P. F. M., Kelly, R., Fatu, C., Furst, D. O., Karsenti, E. and Gautel, M. (2002). Transient association of titin and myosin with microtubules in nascent myofibrils directed by the MURF2 RING-finger protein. *J. Cell Sci.* **115**, 4469-4482.

Pudles, J., Moudjou, M., Hisanaga, S. I., Maruyama, K. and Sakai, H. (1990). Isolation, characterization, and immunological properties of a giant protein from sea urchin egg cytomatrix. *Exp. Cell Res.* **189**, 253-260.

Qi, H., Rath, U., Wang, D., Xu, Y.-Z., Ding, Y., Zhang, W., Blacketer, M. L., Paddy, M. R., Girton, J., Johansen, J. et al. (2004). Megator, an essential coiled-coil protein that localizes to the putative spindle matrix during mitosis in *Drosophila*. *Mol. Biol. Cell* **15**, 4854-4865.

Rath, U., Wang, D., Ding, Y., Xu, Y.-Z., Qi, H., Blacketer, M. J., Girton, J., Johansen, J. and Johansen, K. M. (2004). Chromator, a novel and essential chromodomain protein interacts directly with the putative spindle matrix protein skeletor. *J. Cell. Biochem.* **93**, 1033-1047.

Reuter, R., Panganiban, G. E., Hoffmann, F. M. and Scott, M. P. (1990). Homeotic genes regulate the spatial expression of putative growth factors in the visceral mesoderm of *Drosophila* embryos. *Development* **110**, 1031-1040.

Robinson, R. W. and Snyder, J. A. (2005). Localization of myosin II to chromosome arms and spindle fibers in PtK1 cells: a possible role for an actomyosin system in mitosis. *Protoplasma* **225**, 113-122.

Scholey, J. M., Rogers, G. C. and Sharp, D. J. (2001). Mitosis, microtubules, and the matrix. *J. Cell Biol.* **154**, 261-266.

Shevchenko, A., Wilm, M., Vorm, O. and Mann, M. (1996). Mass spectrometric

sequencing of proteins from silver-stained polyacrylamide gels. *Anal. Chem.* **68**, 850-858.

Silverman-Gavrila, R. V. and Forer, A. (2003). Myosin localization during meiosis I of crane-fly spermatocytes gives indications about its role in division. *Cell Motil. Cytoskeleton* **55**, 97-113.

Spurck, T. P., Stonington, O. G., Snyder, J. A., Pickett-Heaps, J. D., Bajer, A. and Mole-Baier, J. (1990). UV microbeam irradiation of the mitotic spindle. II. Spindle fiber dynamics and force production. *J. Cell Biol.* **111**, 1505-1518.

Trombitás, K. (2000). Connecting filaments: a historical perspective. In *Elastic Filaments of the Cell* (ed. H. L. Granzier and G. H. Pollack), pp. 1-23. New York: Kluwer Academic/Plenum Publishers.

Tsai, M. Y., Wang, S., Heidinger, J. M., Shumaker, D. K., Adam, S. A., Goldman, R. D. and Zheng, Y. (2006). A mitotic lamin B matrix induced by RanGTP required for spindle assembly. *Science* **311**, 1887-1893.

Tskhovrebova, L. and Trinick, J. (2003). Titin: properties and family relationships. *Nat. Rev. Mol. Cell Biol*. **4**, 679-689.

Tskhovrebova, L. and Trinick, J. (2004). Properties of titin immunoglobulin and fibronectin-3 domains. *J. Biol. Chem.* **45**, 46351-46354.

Walker. D. L., Wang, D., Jin, Y., Rath, U., Wang, Y. and Johansen, J. (2000). Skeletor, a novel chromosomal protein that redistributes during mitosis provides evidence for the formation of a spindle matrix. *J. Cell Biol.* **151**, 1401-1411.

Warren, C. M., Krzesinski, P. R. and Greaser, M. L. (2003). Vertical agarose gel electrophoresis and electroblotting of high-molecular-weight proteins. *Electrophoresis* **24**, 1695-1702.

Wernyj, R. P., Ewing, C. M. and Isaacs, W. B. (2001). Multiple antibodies to titin immunoreact with AHNAK and localize to the mitotic spindle machinery. *Cell Motil. Cytoskeleton* **50**, 101-113.

Wilson, P. J., Forer, A. and Leggiadro, C. (1994). Evidence that kinetochore microtubules in crane-fly spermatocytes disassemble during anaphase primarily at the poleward end. *J. Cell Sci.* **107**, 3015-3027.

Wong, R. and Forer, A. (2004). Backward chromosome movement in crane-fly spermatocytes after UV microbeam irradiation of the interzone and a kinetochore. *Cell Biol. Int.* **28**, 293-298.

Zastrow, M. S., Flaherty, D., Benian, G. and Wilson, K. L. (2006). Nuclear titin interacts with A- and B-type lamins in vitro and in vivo. *J. Cell Sci*. **119**, 239-249.

Zhang, Y., Featherston, D., Davis, W., Rushton, E. and Broadie, K. (2000). *Drosophila* D-titin is required for myoblast fusion and skeletal muscle striation. *J. Cell Sci.* **113**, 3103-3115.